ground water

Tracer Mass Recovery in Fractured Aquifers Estimated from Multiple Well Tests

by William E. Sanford[1], Peter G. Cook[2], Neville I. Robinson[3], and Douglas Weatherill[3]

Abstract

Forced-gradient tracer tests in fractured aquifers often report low mass recoveries. In fractured aquifers, fractures intersected by one borehole may not be intersected by another. As a result (1) injected tracer can follow pathways away from the withdrawal well causing low mass recovery and (2) recovered water can follow pathways not connected to the injection well causing significant tracer dilution. These two effects occur along with other forms of apparent mass loss. If the strength of the connection between wells and the amount of dilution can be predicted ahead of time, tracer tests can be designed to optimize mass recovery and dilution. A technique is developed to use hydraulic tests in fractured aquifers to calculate the conductance (strength of connection) between well pairs and to predict mass recovery and amount of dilution during forced gradient tracer tests. Flow is considered to take place through conduits, which connect the wells to each other and to distant sources or sinks. Mass recovery is related to the proportion of flow leaving the injection well and arriving at the withdrawal well, and dilution is related to the proportion of the flow from the withdrawal well that is derived from the injection well. The technique can be used to choose well pairs for tracer tests, what injection and withdrawal rates to use, and which direction to establish the hydraulic gradient to maximize mass recovery and/or minimize dilution. The method is applied to several tracer tests in fractured aquifers in the Clare Valley, South Australia.

Introduction

Forced gradient tracer tests in fractured rock are typically performed to determine field-scale properties of the aquifer that influence ground water flow and solute transport, such as fracture aperture and matrix porosity (e.g., Novakowski et al. 1985; Himmelsbach et al. 1998; Becker and Shapiro 2000; Sanford et al. 2002). However, such tests often record relatively low mass recoveries of the injected tracer, a phenomenon that is frequently poorly explained or unexplained. In the absence of ambient flow, mass recovery of a conservative injected tracer in an equal dipole test (equal injection and extraction rates) should theoretically reach 100%. The presence of an ambient flow, together with practical constraints imposed by limited test duration and finite analytic detection limits, tend to produce mass recoveries <100%. Processes of matrix diffusion and dispersion also contribute to lower mass recoveries, as they tend to produce long tails to the breakthrough curves that are rarely accurately captured. Low mass recovery also arises when tracers subject to degradation or nonreversible sorption are used. Another process that can sometimes lead to extremely low mass recoveries is poor hydraulic connection between injection and extraction wells. This latter process is the subject of the current paper.

In field situations, forced gradient tracer tests are usually performed between two wells by establishing a dipole with either equal or unequal injection/withdrawal rates. In order to maximize tracer recovery, weak dipole configurations, with the withdrawal rate much greater than the injection rate, are often established (Novakowski et al. 1985; Becker and Shapiro 2000; Witthüser et al. 2003). However, if the withdrawal rate is too high, dilution of the injected tracer can lower tracer concentrations,

[1]Corresponding author: Department of Geosciences, Colorado State University, Fort Collins, CO 80523-1482; (970) 491-5929; bills@cnr.colostate.edu

[2]CSIRO Land and Water, Glen Osmond, South Australia.

[3]School of Chemistry, Physics and Earth Sciences, Flinders University, Adelaide, Australia.

Received July 2004, accepted September 2005.

doi: 10.1111/j.1745-6584.2006.00161.x

causing increased uncertainty and even apparent mass loss as concentrations approach and then fall below analytic detection limits.

The premise of this paper is that the mass recovery in highly fractured aquifers largely reflects the degree of connectivity between the injection and withdrawal wells. A few examples of tracer recoveries presented in the literature illustrate this potential problem: Himmelsbach et al. (1998) report on a monopole and a dipole tracer test in a fractured fault zone with mass recoveries of ~70% and 45%, respectively; Sanford et al. (2002) report 28% recovery in a vertical dipole in highly fractured rock; Becker and Shapiro (2000) report recoveries of 83% to 104% in monopole and weak dipole flow fields; and Witthüser et al. (2003) report mass recoveries of ~4% for two tracers injected in a monopole. A technique based on the concept of superposition is developed to use steady-state hydraulic tests in two or more wells to determine the relative strength of connection, termed conductance (see discussion below), between pairs of boreholes and between individual boreholes and distant sources or sinks. The conductance values are used to (1) estimate the fraction of flow leaving the injection well that contributes to the withdrawal well and the fraction of flow entering that withdrawal well that comes from the injection well; (2) predict mass recovery and dilution at the withdrawal well in the absence of other forms of mass loss; and (3) choose well pairs and, in the case of weak dipoles, which direction to establish the hydraulic gradient to maximize mass recovery and minimize dilution. The method is successfully applied to several field-scale tracer tests.

Model Development

Before performing tracer tests in fractured systems, it is usually desirable to first perform hydraulic tests in the wells to identify connections. In fractured aquifers, it is possible that fractures that intercept one well may not intercept other wells. In modeling fluid flow and solute transport through a network of channels, Moreno and Neretnieks (1993) and, in a similar manner, Dershowitz and Fidelibus (1999) assigned a hydraulic conductance to individual channels (fractures) in the network, which they define as the ratio between the flow in a channel and the hydraulic head difference between its ends. We apply this concept to hydraulic tests and divide the flow into or out of a well into several components using superposition, where for each flow component:

$$Q = C\Delta h \tag{1}$$

where Q is the volumetric flow rate, C is the conductance (or strength of the connection), and Δh is the difference in hydraulic heads. It is clear by comparing Darcy's law

$$Q = AK\frac{\Delta h}{\Delta x} \tag{2}$$

to Equation 1, that $C = AK/\Delta x$. Therefore, the conductance term includes the direct relationship of cross-sectional area (A; i.e., flow geometry) and hydraulic conductivity (K), and the inverse relationship of distance (Δx) and the flow rate for a given head difference. For highly fractured systems, it is difficult to determine any of the individual parameters encompassed in the conductance term, but because the approach is using steady-state hydraulics, the combined effects of these parameters are readily estimated.

If a single, planar fracture forms the connection between the wells, then the conductance value can be decomposed as:

$$C = \frac{w(2b)^3\rho g}{12\mu z} \tag{3}$$

where w is the fracture width, $2b$ is the fracture aperture, z is the distance along the fracture, ρ is the density of water, μ is the viscosity, and g is gravitational acceleration. For a homogeneous confined aquifer, Equation 1 can be compared to the form of the Thiem equation (Schwartz and Zhang 2003) for steady-state radial flow to a well to yield

$$C = \frac{2\pi T}{\ln\left(\frac{r_w}{R}\right)} \tag{4}$$

where T is the aquifer transmissivity, R is the radius of influence (where drawdown is zero), and r_w is the radius of the pumping well. However, for our purposes, the physical representation of the conductance need not be known.

Consider the simple case of two wells located in the same fractured aquifer. During a conventional aquifer test, water will be extracted from one well and drawdown measured in both. At, or near, steady state, the flow rate from the production well can be considered as a sum of the contributions of flow from all fractures that are intersected by the pumped well, some of which connect to the monitoring well. Likewise, there are fractures intersected by the monitoring well, which are not connected to the pumped well (Figure 1A).

In modeling flow and estimating permeability using borehole flow logs in heterogeneous fractured systems, Paillet (1998) conceptualized the system as fractures, which contribute flow to the borehole and are connected to different far-field aquifers. Following a similar approach, the system shown in Figure 1A will be considered

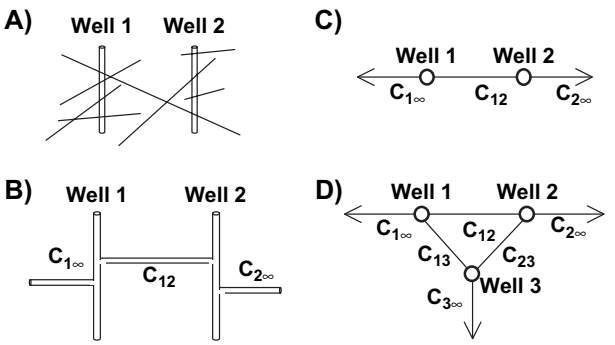

Figure 1. Schematic illustrating the meaning of conductance. (A) Fracture system (in cross section), (B) representation of conductance (cross section), (C) two-well representation of conductance (plan view), (D) three-well representation of conductance (plan view).

as three separate conduits, each with its own conductance: a conduit that connects each well, and a conduit for each well that represents the fractures that one well intersects that the other well does not. The conduits, which are not connected to the other well are considered to be connected to an infinite water source (Figures 1B, 1C; Paillet 1998). From hereon, these conduits will be referred to as connections to infinity. It should be noted that in systems with more than two wells, the conductance values between any two wells and between the wells and infinity may be influenced (increased) by additional bores that provide connections between previously isolated fracture sets. However, this is only of concern if we attempt to give physical meaning to the conductance values.

The drawdowns in each well are controlled by the conductance values of the various conduits. The flow rate through each conduit can be represented by Equation 1, and the flow rate at each well is the sum of the flow in the conduits connected to the well.

The model will be developed initially for two wells. It is assumed that the natural gradient is negligible compared to the imposed gradient, the hydraulic head at infinity (or radius of influence) is constant in time, the flow field has approached steady state, fracture apertures do not change with differing pumping rates, no hydraulic boundaries are encountered, and fractures are not drained or filled. The strictness of these assumptions will be discussed later in the paper. In the following, flow rates from withdrawal wells are considered as positive values, injection rates as negative, lowering of water level as positive drawdown, and raising of water level as negative drawdown.

To determine the conductance values, it is necessary to perform two hydraulic tests. The flow into or out of each well is partitioned into flow to or from infinity and flow between each well. For the first test, the flow rate for well 1 is given by

$$Q_{11} = C_{1\infty} H_{11} + C_{12}(H_{11} - H_{12}) \tag{5}$$

and the flow rate for well 2 is

$$Q_{12} = C_{2\infty} H_{12} + C_{12}(H_{12} - H_{11}) \tag{6}$$

For the second hydraulic test, the equations are

$$Q_{12} = C_{2\infty} H_{12} + C_{12}(H_{12} - H_{11}) \tag{7}$$

$$Q_{22} = C_{2\infty} H_{22} + C_{12}(H_{22} - H_{21}) \tag{8}$$

where Q_{ij} is the pumping rate for test i and well j, H_{ij} is the drawdown in well j as a result of pumping test i, $C_{1\infty}$ is the conductance of well 1 to infinity, $C_{2\infty}$ is the conductance of well 2 to infinity and C_{12} is the conductance of the connection between wells 1 and 2 (Figures 1B, 1C). (For an equal-strength dipole test, $Q_{i1} = -Q_{i2}$.) The possible combinations of flow geometries are shown in Figure 2.

$C_{1\infty}$ and $C_{2\infty}$ can be solved independently from C_{12} by forming two equations from the addition of Equations 5 to 6 and Equations 7 to 8. There remain the original four equations to determine C_{12}, each of which will technically suffice. It is a numerically more robust procedure to solve the overdetermined system for all three conductances in a least squares regression procedure. This amounts to solving the matrix equation for the conductance values

$$[H]^{\mathrm{T}}[H][C] = [H]^{\mathrm{T}}[Q] \tag{9}$$

where $[H]$, $[C]$, and $[Q]$ are the respective matrices of drawdowns, conductances, and pumping rates, and $[H]^{\mathrm{T}}$ is the matrix transpose of $[H]$.

To use the previous equations, it is necessary to hydraulically test both wells in some manner. This can be a single-well test in each well (flow rate for a nonpumping well is zero), a single-well test in one well along with a dipole test (equal or unequal strength), and two dipole tests, where at least one must be of unequal strength (if both are of unequal strength, the second test must have flow rates that are in different ratios to the first). Drawdowns must be measured in each well for each test.

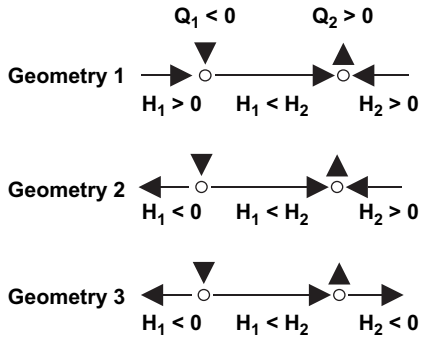

Figure 2. Schematic representations of the three flow geometries discussed in the text for different values of the injection/withdrawal rate ratio. When $H_1 = 0$, there is no flow to or from infinity at well 1. When $H_2 = 0$, there is no flow to or from infinity at well 2.

Recovery of Injected Water and Potential Dilution

The conductance values determined from the hydraulic tests can be used to estimate the fraction of injection water that actually makes it to the withdrawal well and the fraction of the withdrawn water that is injected water. For a dipole, three flow geometries can be envisioned (Figure 2): (1) the withdrawal rate is so great that all water injected is removed at the extraction well while mixing with water coming from infinity; (2) the injection and withdrawal rates are such that the injection flow can be divided between what flows to the extraction well, and what flows to infinity and water extracted can be divided between what comes from the injection well and what comes from infinity; and (3) the injection rate is so great that all water extracted comes from the injection well, while the remainder of the injected water flows out to infinity. Subsequently, the conditions necessary for the transition from one flow geometry to another will be determined from the conductance values, which will allow an estimation of the fraction of the injected water that is recovered and the potential dilution at the withdrawal well.

The injection flow can be divided between what flows to the extraction well and what flows to infinity. Consider a dipole test such that:

$$Q_1 = -RQ_2 \tag{10}$$

where R is the ratio of magnitude of the injection rate to magnitude of the withdrawal rate (for a dipole of equal strength, $R = 1$). For notational simplicity, we suppose that well 1 is the injection well and well 2 is the extraction well and omit the subscripts for test number, so that $Q_1 \leq 0$ is the injection flow rate, $Q_2 \geq 0$ is the withdrawal flow rate, and H_1 and H_2 are the drawdowns in the injection well and withdrawal well, respectively. The flow rate between wells 1 and 2 is given by

$$q_{12} = C_{12}(H_1 - H_2) \tag{11}$$

The transition from flow geometries 1 to 2 occurs when the magnitude of the injection rate is such that there is no water table rise or drawdown in the injection well, $H_1 = 0$, and there is no flow to infinity and all the injected water goes to the extraction well. The value of R, say R_0, at which this transition occurs is found using $H_1 = 0$ with Equations 5 and 6 and then Equation 10 to yield

$$R_0 = \frac{C_{12}}{C_{2\infty} + C_{12}} \tag{12}$$

When $R < R_0$, the withdrawal rate is great enough to produce a net decrease in water level in the injection well, and flow between the injection and withdrawal wells is a sum of all flow being injected and the flow from infinity to the injection well (geometry 1 in Figure 2). As $Q_1 \rightarrow 0$, the geometry approaches that of a convergent monopole.

The transition from flow geometries 2 to 3 occurs when the withdrawal rate is such that there is no net change in water level in the withdrawal well, $H_2 = 0$, and there is no flow from infinity and all extracted water comes from the injection well. The value of R at which this occurs, say R_1, is found by using $H_2 = 0$ with Equations 5 and 6 and then Equation 10 to give

$$R_1 = \frac{C_{12} + C_{1\infty}}{C_{12}} \tag{13}$$

When $R > R_1$, the injection rate is great enough to produce a net increase in water level in the extraction well, resulting in no withdrawal water coming from infinity, and all the water being withdrawn is water that is being injected (geometry 3 in Figure 2). As $Q_2 \rightarrow 0$, the geometry approaches that of a divergent monopole.

Flow geometry 2 occurs when $R_0 \leq R \leq R_1$ (Figure 2), which results in both an increase in water level in the injection well ($H_1 < 0$) and a decrease in water level in the withdrawal well ($H_2 > 0$).

Potential Mass Recovery

An estimate of the maximum amount of an injected mass that can be recovered during a tracer test can be made from the fraction, F, of the injection flow rate that contributes to the withdrawal rate, defined as

$$F = \frac{q_{12}}{Q_1} \tag{14}$$

The fraction F can be considered as the maximum mass recovery that can be expected due to the impact of interwell connectivity in the absence of other physical and chemical attenuation factors. Explicit values of F in terms of conductances and critical values of R can be derived from Equations 5, 6, 10, and 12. For the values of R between R_0 and R_1, Equation 14 can be solved by algebraically combining Equations 5 and 6, resulting in

$$F = 1 \quad \text{for } R \leq R_0$$

$$F = \frac{C_{12}C_{1\infty} + RC_{12}C_{2\infty}}{R(C_{12}C_{1\infty} + C_{1\infty}C_{2\infty} + C_{12}C_{2\infty})} \quad \text{for } R_0 \leq R \leq R_1$$

$$F = \frac{1}{R} \quad \text{for } R \geq R_1 \tag{15}$$

It is important to note here that for a dipole of equal strength ($R = 1$), the fraction of the flow between the two wells (F) is the same regardless of which is the injection and which is the withdrawal well. However, for a dipole of unequal strength, the value of F between the two wells is dependent on which is used for injection and withdrawal as reflected by the presence of the R term in the numerator of Equation 15.

Dilution at the Withdrawal Well

The previous equations illustrate that potential mass recovery is related to the conductance values, ratio of injection to withdrawal rates, and the direction of flow. A significant impact is expected on concentrations of tracer recovered, with dilution potentially being quite significant. A dilution factor, D_F, can be defined as the contribution of injection water to the total withdrawal

$$D_F = \frac{-q_{12}}{Q_2} = RF \tag{16}$$

Relationship of R to F and D_F

The relationships between the flow ratio, R, the potential fraction of injected water recovered, F, and the dilution factor at the withdrawal well, D_F, are illustrated in Figure 3 with all conductance values normalized to C_{12}, with $C_{2\infty} = C_{12} = 1$ and $C_{1\infty} = 0.1$, 1.0, and 10. For each case illustrated, when $R \leq R_0$, all of the water injected is recovered, so $F = 1$. The dilution factor increases linearly as $R \rightarrow R_0$, as more of the recovered water is supplied by the injection well (Figure 3). When $R > R_0$, some of the injected water now is flowing to infinity away from the withdrawal well and $F < 1$, yet more of the recovered water is coming from the injection well, resulting in less dilution (D_F increases; Figure 3). When $R \geq R_1$, all water being withdrawn is coming from the injection well, so there is no dilution with water from infinity and $D_F = 1$, but at the same time, more of the water being injected is flowing out to infinity causing F to decrease (Figure 3). Therefore, when $R \leq R_0$, mass recovery is at a maximum while there can be significant dilution in the withdrawal well (Figure 3); when $R \geq R_1$,

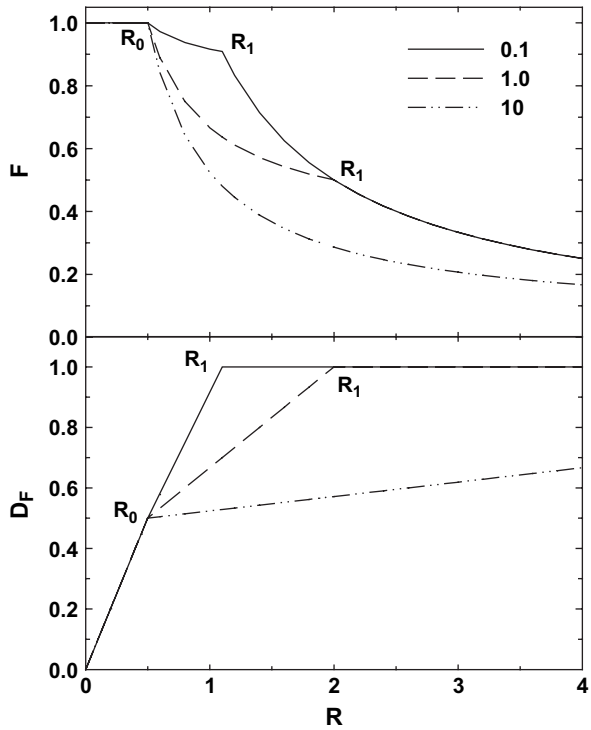

Figure 3. Relationship of fraction of mass recovered (F) and the dilution factor (D_F) to injection-withdrawal rate ratio (R) for $C_{1\infty} = 0.1$, 1.0, and 10 with $C_{12} = C_{2\infty} = 1$. Conductance values are normalized to C_{12}. R_0 and R_1 are transition values as defined in the text.

the effects of dilution are at a minimum, while there can be considerable mass loss.

The values of R_0 and R_1 are controlled by the relationship of the three conductance values. The value of R_0 is the same for all examples shown in Figure 3 but the values of R_1 are quite different for the three values of $C_{1\infty}$ used: $R_1 = 1.1$ for $C_{1\infty} = 0.1$, $R_1 = 2.0$ for $C_{1\infty} = 1.0$, and $R_1 = 11$ for $C_{1\infty} = 10$. For the latter value of $C_{1\infty}$, the injection rate would need to be at least 11 times that of the withdrawal rate to get no dilution, but >90% of the injected water would not be recovered.

As illustrated in Figure 3, there is a trade-off between mass recovery (F) and dilution (D_F) that is a function of the conductance values and the ratio of the injection to withdrawal rates (R). If it is desired to maximize mass recovery, then it would be best to use the condition where $R \leq R_0$. However, as the value of R decreases relative to R_0, the amount of dilution increases (Figure 3). If it is desired to minimize dilution, then it would be best to use the condition where $R \geq R_1$. In addition, as the value of R increases relative to R_1, the amount of mass loss increases (Figure 3). In many cases, the optimal pumping ratio to use for mass recovery and dilution may be a value of $R = 1$ (equal-strength dipole).

Three-Well Solution

In some situations, it will be necessary for the use of equations to calculate conductance values using three wells. The approach for determining the conductance values for a three-well problem is similar to that used for the two-well problem: assume flow through each well is a sum of the flow from infinity and the flows from each of the other two wells (Figure 1D):

$$Q_1 = C_{1\infty}H_1 + C_{12}(H_1 - H_2) + C_{31}(H_1 - H_3) \quad (17)$$

$$Q_2 = C_{2\infty}H_2 + C_{12}(H_2 - H_1) + C_{23}(H_2 - H_3) \quad (18)$$

$$Q_3 = C_{3\infty}H_3 + C_{31}(H_3 - H_1) + C_{23}(H_3 - H_2) \quad (19)$$

To solve the three-well problem, it is necessary to perform three separate hydraulic tests involving all three wells. Equations 17 to 19 would be written for all three hydraulic tests. The values of $C_{1\infty}$, $C_{2\infty}$, and $C_{3\infty}$ can be found by summing together the equations for each test, but it is numerically more robust solving for all six conductances from a 9×6 overdetermined matrix. For hydraulic testing, different combinations of tests can be used (remembering that heads need to be measured in each well for each test): 3 single-well tests; a single-well test followed by two dipole tests using the single well as one of the poles; dipole tests between all three; etc. One situation where this method is useful is when there are three or more wells at a site. One well can be used in a single-well test, followed by dipoles created with two other wells using the well tested as one of the poles. With this method, the conductance between the other wells not used for single-well testing can be determined.

Equivalence of Two-Well and Three-Well Networks in a Dipole Test

When the conductance values are determined using three wells, the two-well mass balance equation can be used to determine well pairs that would give the best mass recovery for a dipole tracer test. To do so, the conductance values including the third well need to be incorporated for the mass balance calculations. For a dipole between well 1 and well 2, the equivalent conductances are found by setting $Q_2 = -Q_1$ in Equation 18 and $Q_3 = 0$ in Equation 19, and solving Equations 17 to 19 simultaneously to arrive at

$$C'_{1\infty} = C_{1\infty} + \frac{C_{31}C_{3\infty}}{C_{3\infty} + C_{31} + C_{23}} \quad (20)$$

$$C'_{2\infty} = C_{2\infty} + \frac{C_{23}C_{3\infty}}{C_{3\infty} + C_{31} + C_{23}} \quad (21)$$

$$C'_{12} = C_{12} + \frac{C_{31}C_{23}}{C_{3\infty} + C_{31} + C_{23}} \quad (22)$$

These values are used in Equations 13 to 15 by substituting the corresponding unprimed term. Sets of three conductance values for dipoles between wells 2 and 3 and wells 3 and 1 are obtained from Equations 20, 21, and 22 by cyclic symmetry of the conductance subscripts;

i.e., for wells 2 and 3, the subscripts in the previous equations are altered: $1 \rightarrow 2$, $2 \rightarrow 3$, and $3 \rightarrow 1$.

Illustrative Applications

In this section, the previous equations will be applied to theoretical examples to illustrate how they can be used to guide the design and implementation of field-scale tracer tests in fractured systems to optimize mass recovery. The discussion to follow is based on using a conservative tracer with no other types of mass loss except for flow along conduits not connected to the withdrawal well and apparent loss due to dilution. Mass loss by other processes, as described earlier, will result in even less mass recovery.

Determination of Well Pairs to Maximize Mass Recovery

The analysis presented previously can be used to choose well pairs in order to maximize mass recovery for tracer tests performed in a flow field of a dipole of equal strength. For this example, there are three wells (1, 2, and 3) in the field site and hydraulic tests have been performed with the conductance values given in Table 1.

Using these conductance values in Equations 20 to 22, the mass recovery between the possible well pairs for tests with dipoles of equal strength ($R = 1$) can be estimated from Equation 15, resulting in $F_{12} = 0.35$, $F_{13} = 0.88$, and $F_{23} = 0.13$ (with F_{ij} being the recovery estimates between wells i and j). The analysis indicates that the best wells to use to optimize mass recovery are wells 1 and 3 and since $R = 1$ and $D_F = 0.88$.

Direction for Weak Dipole

The technique can be used to identify the best direction to use if it is decided to conduct an unequal-strength dipole tracer test. We will use the example in Table 1 for the dipole between wells 2 and 3. The estimated fraction of the injected water recovered for a dipole of equal strength is 0.13, regardless of flow direction. If it was decided that a weak dipole should be used, with the injection rate being 10% of the withdrawal rate ($R = 0.1$), the estimated recovery is dependent upon the direction of flow. If injection is in well 2 and withdrawal from well 3, then $F = 0.91$. If the direction is reversed, then $F = 0.54$. Since $R = 0.1$, the dilution factors are 0.09 and 0.054, respectively. For the weak dipole, it is advantageous to choose the direction predicting the greatest mass recovery and least amount of dilution as given by Equation 16. Quantification of the degree of dilution can also assist in determining the concentration of tracer to be injected.

Application to Field Examples

Two field sites were chosen to test the applicability of the approach. Both sites are in the Clare Valley of South Australia, located ~100 km north of Adelaide. Numerous investigations into ground water flow through fractured rocks have been done in the area (Cook et al. 1999; Cook and Simmons 2000; Sanford et al. 2002). At both locations, hydraulic tests were performed in order to calculate conductance values, and tracer tests were carried out using dipoles of equal strength. The Wendouree site is underlain by the fractured Auburn Dolomite of Proterozoic age that consists mainly of thin-bedded dolomite with dark slate and siltstone present (Morton et al. 1998). At this site, the hydraulic and tracer tests were performed vertically between a nest of three piezometers. The Duncan site is located ~3 km southwest of the Wendouree site and is underlain by the fractured Undalya Quartzite (Morton et al. 1998). At this site, the hydraulic and tracer tests were performed subhorizontally between piezometers.

Methods

Tracer tests were conducted at both sites using bromide and dissolved helium. The methods are described in detail in Sanford et al. (2002) for a tracer test at the Wendouree site. The other tracer tests are unpublished but followed the same procedures. All tests were done in the flow field of a dipole of equal strength. Once the flow field was established (flow rates ranging from 2.7×10^{-5} to 1.0×10^{-4} m^3/s (1.6 to 6.0 L/min)), a pulse of tracer-tagged water was added (lasting 49 to 80 min), then followed by tracer-free water for 9 to 27.5 h. Samples were collected at the withdrawal well and analyzed for tracer concentrations following the procedures outlined in Sanford et al. (2002). In some cases, multiple tracers were used to investigate the effects of matrix diffusion on solute transport in the region.

The hydraulic tests were performed with a submersible pump using flow rates similar to those that were used for the tracer tests. All tests were continued until

Table 1
Conductance Values (m^2/s) Used for Illustrative Examples. Values Represent Data from a Three-Well Solution. F Values Are Those for a Dipole of Equal Strength ($R = 1$)

Conductance		Dipole 1-2		Dipole 1-3		Dipole 2-3	
$C_{1\infty}$	5×10^{-5}	$C'_{1\infty}$	5.3×10^{-5}	$C'_{1\infty}$	5.7×10^{-5}	$C'_{2\infty}$	3.4×10^{-5}
$C_{2\infty}$	3×10^{-5}	$C'_{2\infty}$	3.1×10^{-5}	$C'_{3\infty}$	7.3×10^{-7}	$C'_{3\infty}$	1.8×10^{-5}
$C_{3\infty}$	1×10^{-5}	C'_{12}	1×10^{-5}	C'_{13}	5.2×10^{-6}	C'_{23}	1.8×10^{-6}
C_{12}	1×10^{-5}	F_{12}	0.35	F_{13}	0.88	F_{23}	0.13
C_{13}	5×10^{-6}						
C_{23}	1×10^{-6}						

drawdown ceased. For the dipole tests, the discharge end of the submersible pump was placed into a different piezometer.

Wendouree Results

Three nested piezometers (P4, P5, and P6) were used at the Wendouree site. The vertical piezometers are constructed of 50-mm-diameter polyvinyl chloride installed in a 250-mm-diameter bore. Each piezometer has a screened interval of 3 m with P4 at 27- to 30-m depth, P5 at 18- to 21-m depth, and P6 at 9- to 12-m depth. The screened sections are separated by bentonite and cement plugs. At this site, a single-well hydraulic test was performed in each piezometer with equal pumping rates of 8.3×10^{-5} m^3/s (5.0 L/min). The drawdowns resulting from the hydraulic tests at Wendouree are given in Table 2. Conductance values were calculated using the three-well solution (Equations 17, 18, and 19) and are given in Table 3.

A tracer test was conducted in 1999 between P5 and P4 (Sanford et al. 2002). In this test, a steady-state dipole with flow rates of 7.8×10^{-5} m^3/s (4.7 L/min) was used and bromide and helium were the tracers. Following the hydraulic tests discussed previously, another tracer test using bromide and helium was conducted between P6 and P5 at a flow rate of 2.7×10^{-5} m^3/s (1.6 L/min). As helium has a smaller aqueous diffusion coefficient than bromide, the use of dual tracers allowed investigation of the effects of matrix diffusion. Breakthrough of helium and bromide in both tests clearly show effects of matrix diffusion (Figure 4A).

The Wendouree conductance values were used in Equations 20 to 22 and Equation 15 to determine F values for the tests from P5 to P4 and P6 to P5. It is estimated that for a dipole of equal strength, 29% of the injected flow into P5 should be recovered in P4 and 54% of the injected flow into P6 should be recovered in P5. For the tracer test from P5 to P4 run in 1999, the mass recovery of bromide was 24% and of helium was 21% (Figure 4B), which compares well with the 29% recovery predicted from the hydraulic tests performed in 2004. For the tracer test from P6 to P5, 55% of the mass of injected bromide and 50% of helium was recovered (Figure 4B), again close to that estimated from the conductance values. Note that for both tracer tests, the mass recovery curves were beginning to plateau when the tracer concentrations fell below the detection limits.

Duncan Results

The Duncan site has three nests of piezometers (designated C, M, and S), which are aligned north-south. The M piezometers are located 6.2 m south of the C piezometers, and the S piezometers are located 12.5 m south of the M piezometers. Each nest consists of 5 piezometers with 3-m screen lengths at depths of 10 to 13 m, 20 to 23 m, 30 to 33 m, 40 to 43 m, and 50 to 53 m, separated by bentonite and cement plugs. They are numbered from 1 to 5 with 1 being the deepest and 5 being the shallowest. The topography of the site is relatively flat, so the corresponding depths for each nest are at the same elevation.

At the Duncan site, single-well and equal-strength dipole hydraulic tests were performed: a single-well test was performed in M3 ($Q = 8.3 \times 10^{-5}$ m^3/s [5.0 L/min]) and dipoles were established from M3 to C3 ($Q = 1.0 \times 10^{-4}$ m^3/s [6.0 L/min]), C3 to M3 ($Q = 6.7 \times 10^{-5}$ m^3/s [4.0 L/min]), and M3 to S3 ($Q = 1.0 \times 10^{-4}$ m^3/s [6.0 L/min]). The drawdowns from these tests are given in Table 2. The conductance values for M3 to C3 were calculated using tests 4 and 5 (Table 2), conductance values for C3 to M3 were calculated using tests 4 and 6 (Table 2), and the conductance values for M3 to S3 were calculated using tests 4 and 7 (Table 2). All the conductance values for the Duncan site are given in Table 3. Note that the estimated value of $C_{M3\infty}$ is essentially the same for the tests from C3 to M3 and M3 to C3, but the value is different for the M3 to S3 test due to the different directions.

A series of tracer tests using bromide were conducted between piezometers C3 and M3 at different flow rates. A single test was also conducted in the reverse direction (from M3 to C3), and one test was conducted between M3 and S3. All of these tracer tests were performed

Table 2
Steady-State Drawdown Values Resulting from Hydraulic Testing at the Wendouree and Duncan Sites and the Different Test Configurations. Negative Values of Drawdown Indicate Water Level Rise in the Piezometer

		Drawdown (m)			
		Wendouree Data			
Test	Hydraulic Test Configuration	P4	P5	P6	Pumping Rate (m^3/s)
1	P4 (single well)	0.34	0.07	0.03	8.3×10^{-5}
2	P5 (single well)	0.07	0.50	0.13	8.3×10^{-5}
3	P6 (single well)	0.03	0.12	0.25	8.3×10^{-5}
		Duncan Data			
		M3	C3	S3	
4	M3 (single well)	5.3	0.77	0.44	8.3×10^{-5}
5	In M3–out C3 (equal dipole)	−6.0	0.74	—	1.0×10^{-4}
6	In C3–out M3 (equal dipole)	4.42	−0.51	—	6.7×10^{-5}
7	In M3–out S3 (equal dipole)	−6.38	—	1.86	1.0×10^{-4}

Table 3
Conductance Values (m^2/s) at the Wendouree and Duncan Sites Based on Measured Drawdown Values Given in Table 2

	Wendouree		Duncan	
Three-well solution	$C_{4\infty} = 2.1 \times 10^{-4}$	$C_{45} = 2.9 \times 10^{-5}$	M3 to C3	$C_{C3\infty} = 5.0 \times 10^{-5}$
	$C_{5\infty} = 6.6 \times 10^{-5}$	$C_{46} = 1.6 \times 10^{-5}$		$C_{M3\infty} = 6.3 \times 10^{-6}$
	$C_{6\infty} = 2.8 \times 10^{-4}$	$C_{56} = 8.1 \times 10^{-5}$		$C_{M3\text{-}C3} = 7.7 \times 10^{-6}$
Two-well solution	P5 to P4	$C'_{5\infty} = 1.3 \times 10^{-4}$	C3 to M3	$C_{C3\infty} = 5.2 \times 10^{-5}$
		$C'_{4\infty} = 2.2 \times 10^{-4}$		$C_{M3\infty} = 7.0 \times 10^{-6}$
		$C'_{54} = 3.2 \times 10^{-5}$		$C_{C3\text{-}M3} = 8.7 \times 10^{-6}$
	P6 to P4	$C'_{6\infty} = 2.9 \times 10^{-4}$	M3 to S3	$C_{M3\infty} = 1.2 \times 10^{-5}$
		$C'_{5\infty} = 9.0 \times 10^{-5}$		$C_{S3\infty} = 3.9 \times 10^{-5}$
		$C'_{65} = 8.3 \times 10^{-5}$		$C_{M3\text{-}S3} = 3.3 \times 10^{-6}$

before the development of the technique presented in this paper. One of the tracer tests between C3 and M3 also included the use of helium, and the effect of matrix diffusion is evident in the separation of the bromide and helium (Figure 5A). The breakthrough curves of the other three tracer tests are given in Figure 6A.

Based on conductance values determined from the hydraulic tests, the mass recovery for an equal-strength dipole between C3 and M3 (either direction) is estimated to be 58%. The actual mass recoveries for the tracer tests from C3 and M3 were 52% of the bromide with a flow rate of 1.0×10^{-4} m^3/s (6.0 L/min; Figure 6B) and 52% bromide and 39% helium with a flow rate of 3.8×10^{-5} m^3/s (2.3 L/min; Figure 5B). For the tracer test from M3 to C3, the actual recovery was 36% of the bromide with a flow rate of 1.0×10^{-4} m^3/s (6.0 L/min; Figure 6B). The mass recovery curve for the M3 to C3 test (Figure 6B) clearly shows that the tracer test was stopped too early. Note that the mass recovery curves had not yet flattened for a few of the tests when the concentrations fell below the detection limit.

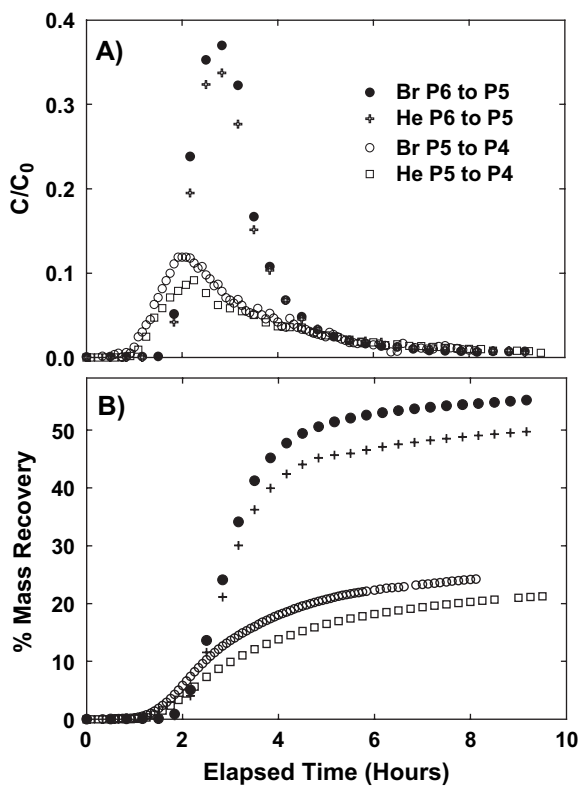

Figure 4. Results of the tracer tests at the Wendouree site. (A) Breakthrough curves, (B) mass recovery curves.

For the one test performed from M3 to S3, the estimated mass recovery is 27%, with the actual mass recovery being 2% for a flow rate of 1.0×10^{-4} m^3/s (6.0 L/min; Figure 6B). The reasons for the low recovery for the M3 to S3 test are not clear. The mass recovery curve shows that the tracer concentration was beginning to increase. In addition, for this configuration, the dilution factor at the withdrawal well is 0.27. Therefore, the low recovery was most likely a combination of stopping the test too soon and dilution at the withdrawal well, both coupled with the effects of matrix diffusion and dispersion.

Discussion

The analyses of aquifer tests presented above can be used to determine the strength of connections between wells in highly fractured aquifers. The procedure is essentially calculating the fraction of stream tubes leaving the injection well that connect to the withdrawal well and then calculating the fraction that these stream tubes contribute to the flow entering the withdrawal well. Because of the many processes of solute transport which result in actual or apparent mass loss, such as sorption, matrix diffusion, dispersion, degradation or decay of the tracer, apparent loss by dilution, stopping the test too early, ambient flow and tracer-tagged water following fractures that are not connected to the withdrawal well, this technique will allow for maximizing the hydraulic connections between wells to use in a tracer test, thereby optimizing potential tracer recovery and amount of dilution. The results of the analyses can be used to identify well pairs to use for equal-strength dipoles and, for tracer tests performed under other types of forced gradient conditions (monopoles and weak dipoles), determine which wells to use for injection and withdrawal and what pumping rates to use to get maximum tracer recovery and minimal dilution.

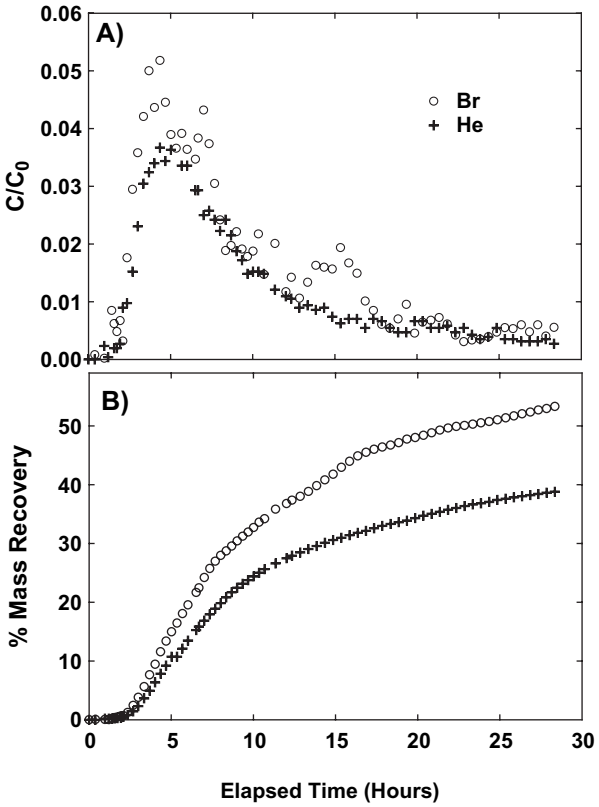

Figure 5. Results of tracer tests at the Duncan site. (A) Breakthrough curves for bromide and helium from the test between C3 and M3 at 2.3 L/min, (B) mass recovery curves.

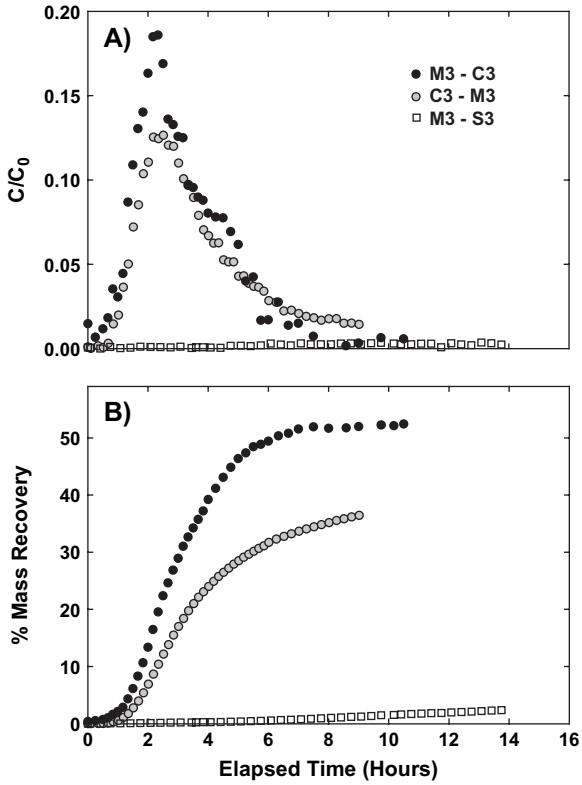

Figure 6. Results of tracer tests at the Duncan site. (A) Breakthrough curves for bromide between C3 and M3, M3 and C3, and M3 and S3, each at 6 L/min. (B) Mass recovery curves.

Limitations

In the development of the technique it is assumed that the natural gradient is negligible compared to the imposed gradient, the hydraulic head at infinity (or radius of influence) is constant in time (no drawdown), the flow field has approached steady state, fracture apertures do not change with differing pumping rates, no hydraulic boundaries are encountered, and fractures are not drained or filled. Clearly, these situations will affect the calculated values of conductance, and hence cause some errors in the predicted mass recoveries and tracer dilutions. In the case of an ambient flow field, the errors can be minimized by creating large head gradients during pumping tests. In the case of draining and/or filling fractures, the errors can be minimized by conducting the hydraulic tests at similar pumping rates as the tracer tests to be conducted. In any case, these situations should be apparent if hydraulic tests are conducted at different pumping rates and drawdowns at the different pumping rates are compared.

Summary

The technique for optimizing mass recovery and dilution during forced gradient tracer tests in fractured aquifers using the results of hydraulic tests has been developed based on the idea of superposition. By hydraulically testing 2 or more wells, the simple mathematical analyses can be used to determine the strength of connection (conductance) between the wells, which can then be used to estimate mass recovery and dilution during forced gradient tracer tests. For tracer tests using other than equal-strength dipoles, the mass recovery is dependent upon the direction of flow and the ratio of injection/withdrawal rates. Low mass recovery for tracer tests in highly fractured rock is often reported in the literature. A significant portion of the loss could be the result of tracer being injected into fractures which do not connect to the withdrawal well and/or significant dilution at the withdrawal well by tracer-free water. Having an estimate of maximum mass recovery, in the absence of other forms of mass loss, and potential dilution before the tracer test is performed will provide information to use in modeling to allow for optimization of tracer concentrations, flow rates for injection and withdrawal, flow directions, and total duration of the test.

Acknowledgments

The authors thank Fred Day-Lewis and the anonymous referees for their technical comments, which considerably improved the manuscript.

References

Becker, M.W., and A.M. Shapiro. 2000. Tracer transport in fractured crystalline rock: Evidence of nondiffusive breakthrough tailing. *Water Resources Research* 36, no. 7: 1677–1686.

Cook, P.G., A.J. Love, and J.C. Dighton. 1999. Inferring ground water flow in fractured rock from dissolved radon. *Ground Water* 37, no. 4: 606–610.

Cook, P.G., and C.T. Simmons. 2000. Using environmental tracers to constrain flow parameters in fractured rock aquifers: Clare Valley, South Australia. In *Dynamics of Fluids in Fractured Rock*, ed. B. Faybishenko, P.A. Witherspoon, and S.M. Benson, 337–347. American Geophysical Union, Washington, D.C.

Dershowitz, W.S., and C. Fidelibus. 1999. Derivation of equivalent pipe network analogues for three-dimensional discrete fracture networks by the boundary element method. *Water Resources Research* 35, no. 9: 2685–2691.

Himmelsbach, T., H. Hotzl, and P. Maloszewski. 1998. Solute transport processes in a highly permeable fault zone of Lindau Fractured Rock Test Site (Germany). *Ground Water* 36, no. 5: 792–800.

Moreno, L., and I. Neretnieks. 1993. Fluid flow and solute transport in a network of channels. *Journal of Contaminant Hydrology* 14, no. 3–4: 163–192.

Morton, D., A.J. Love, D. Clarke, R. Martin, P.G. Cook, and K. McEwan. 1998. Clare Valley groundwater resources. Progress Report 1: Hydrogeology, drilling and groundwater monitoring. Report Book 98/00015. Primary Industries and Resources South Australia, Adelaide, Australia.

Novakowski, K.S., G.B. Evans, D.A. Lever, and K.G. Raven. 1985. A field example of measuring hydrodynamic dispersion in a single fracture. *Water Resources Research* 21, no. 8: 1165–1174.

Paillet, F. 1998. Flow modeling and permeability estimation using borehole flow logs in heterogeneous fractured formations. *Water Resources Research* 34, no. 5: 997–1010.

Sanford, W.E., P.G. Cook, and J.C. Dighton. 2002. Analysis of a vertical dipole tracer test in highly fractured rock. *Ground Water* 40, no. 5: 535–542.

Schwartz, F.W., and H. Zhang. 2003. *Fundamentals of Ground Water*. Hoboken, New Jersey: Wiley.

Witthüser, K., B. Reichert, and H. Hötzl. 2003. Contaminant transport in fractured chalk: Laboratory and field experiments. *Ground Water* 41, no. 6: 806–815.